Received: 24 March 2024 | Revised: 2 July 2024 | Accepted: 20 August 2024

DOI: 10.4218/etrij.2024-0142

SPECIAL ISSUE

ETRI Journal WILEY

Free-space quantum key distribution transmitter system using WDM filter for channel integration

Minchul Kim | **Kyongchun Lim** | **Joong-Seon Choe** | **Byung-Seok Choi** | **Kap-Joong Kim** | **Ju Hee Baek** | **Chun Ju Youn**

Quantum Technology Research Division, Electronics and Telecommunications Research Institute, Daejeon, Republic of Korea

Correspondence
Chun Ju Youn, Quantum Technology Research Division, Electronics and Telecommunications Research Institute, Daejeon, Republic of Korea.
Email: cjyoun@etri.re.kr

Funding information
This work was supported by Institute of Information & Communications Technology Planning & Evaluation (IITP) grants funded by the Korean government (MSIT) (RS-2019-II190005, Technology development of transmitter and receiver integrated module in a polarization-based free-space quantum key distribution for short-range low-speed moving quantum communication), (RS-2020-II200890, Development of trusted node core and interfaces for the interoperability among QKD protocols), and (RS-2022-II221014, Technology development of lightweight free space quantum repeating platform).

Abstract

In this study, we report a transmitter system for free-space quantum key distribution (QKD) using the BB84 protocol, which does not require an internal alignment process, by using a wavelength-division multiplexing (WDM) filter and polarization-encoding module. With a custom-made WDM filter, the signals required for QKD can be integrated by simply connecting fibers, thus avoiding the laborious internal alignment required for free-space QKD systems using conventional bulk-optic setups. The WDM filter is designed to multiplex the single-mode signals from 785-nm quantum and 1550-nm synchronization channels for spatial-mode matching while maintaining the polarization relations. The measured insertion loss and isolation are 1.8 dB and 32.6 dB for 785 nm and 0.7 dB and 28.3 dB for 1550 nm, respectively. We also evaluate the QKD performance of the proposed system. The sifted key rate and quantum bit error rate are 1.6 Mbps and 0.62%, respectively, at an operating speed of 100 MHz, rendering our system comparable to conventional systems using bulk-optic devices for channel integration.

KEYWORDS
channel integration, free-space quantum communication, free-space quantum cryptography, free-space quantum key distribution, WDM filter

1 | INTRODUCTION

Quantum key distribution (QKD) is a method for distributing encryption keys using the quantum nature of particles in communications. In QKD, keys are typically encoded in the quantum states of photons, such as their polarization, phase, and time-bin.

The fundamental principle behind QKD is that any attempt to eavesdrop on the key exchange disturbs the quantum states in a detectable manner, thereby alerting the communicating parties to the presence of an eavesdropper. This property stems from the principles of quantum mechanics, particularly the Heisenberg uncertainty principle and the no-cloning theorem, which together ensure that quantum information cannot be distinguished or replicated without introducing errors.

Unlike conventional cryptography algorithms that rely on mathematical complexity, QKD guarantees unconditional safety by physically preventing eavesdropping on the intermediate channel between the transmitter and receiver [1]. This feature renders QKD an attractive alternative to conventional cryptosystems because its security

is unchallenged for improving computing performance and developing quantum computers [2].

Among existing QKD platforms, free-space QKD, which uses atmospheric channels as a transmission medium for quantum signals, has been actively investigated for various environments from short to long ranges, owing to its wide applicability. For example, ultralong-distance QKD between low-Earth-orbit satellites and ground stations has been demonstrated [3–5], and studies that have investigated more detailed operating conditions of satellite-to-ground links have also been reported [6–10].

Recent works include a portable QKD ground terminal weighing approximately 100 kg [11], in-laboratory testing of high-speed QKD [12], and a 24-h operation test, including daytime, in a 20-km terrestrial environment [13]. These are considered the foundational steps for the practical implementation of free-space QKD. Other studies have also demonstrated handheld applications for ultrashort-distance environments, such as automatic teller machines (ATMs) and mobile terminals [14, 15]. QKD demonstrations on moving platforms using ground vehicles [16] and airplanes [17, 18] have also been reported.

Recent studies have demonstrated entangled photon distributions in a drone-to-ground environment [19, 20] and investigated an attenuated coherent optical source-based drone-to-drone QKD implementation at a distance of approximately 10 m [21]. In these studies, the sifted key rate and quantum bit error rate (QBER) ranged from 0.15 kbps to 75 kbps and 0.8% to 6.5%, depending on the system and operating environment.

It should be noted that a direct comparison of system capabilities based on the reported key rate and QBER is difficult, as these parameters are largely affected by the operating environment, such as the distance between the transmitter and receiver, time of day, and atmospheric and weather conditions during the test. These factors affect the noise levels and receiving efficiency of quantum signals, which are directly related to the QBER and key rate, resulting in different values even with the same systems.

Meanwhile, related studies have been conducted on both QKD systems and the miniaturization of the required optical components. A compact four-polarization encoding module based on a silica chip for the BB84 protocol and a free-space QKD system employing it have been reported, replacing the bulky waveplates and beam splitters inside the QKD transmitter [22, 23].

In addition, possible security threats caused by exploiting the driving characteristics of multiple laser sources in a QKD transmitter were revealed, and methods for preventing such threats and improving QKD performance were devised [24, 25].

Methods for performing free-space QKD during the daytime by reducing noise in the spectral, spatial, and temporal domains have also been reported. Using these methods, a QBER of 3.47% and a secure key rate of 191 kbps were achieved during the daytime at a system speed of 100 MHz and free-space distance of 275 m [26]. Generally, establishing QKD during the daytime is more challenging than at night because sunlight has a higher intensity than the transmitted quantum key signals.

To implement free-space QKD systems, various signal channels are required, including those for quantum key signals, beam tracking, synchronization, and classical communication. Signals can be effectively transmitted and received through these channels by combining and separating them in the same direction. This process is primarily performed using dichroic mirrors.

However, such a system configuration can be vulnerable to shocks and vibrations caused by the experimental environment and requires delicate and laborious alignment processes. There has been a study that integrated different channels using WDM filters; however, channels with a large wavelength difference are still combined using a dichroic mirror [27].

In this paper, we report the configuration and performance of a free-space QKD transmitter system that does not require internal free-space alignment. This was achieved by using a chip-based polarization-encoding module for generating and integrating four-channel polarization-encoded quantum signals and a wavelength-division multiplexing (WDM) filter for integrating 785-nm quantum and 1550-nm synchronization signals. In addition, we report on an issue related to the use of a WDM filter for multiplexing quantum signals and other channels along with the performance of the fabricated WDM filter.

The proposed QKD system exhibited a QBER of 0.62% and a sifted key rate of 1.6 Mbps at a 100 MHz system driving speed, producing a performance similar to that of our conventional system using bulk-optic components. Compared with the aforementioned sifted key rate and QBER in the related works, we confirm that the proposed QKD system has a comparable performance, considering different operating environments with the related works. By demonstrating that a WDM filter can be used to multiplex QKD channels with large wavelength differences without degrading system performance, we expect that our work will provide meaningful data for miniaturizing QKD systems in related research.

2 | QKD SYSTEM CONFIGURATION

Figure 1 shows the configurations of the transmitter and receiver sides of the implemented free-space QKD system. The polarization-based BB84 protocol was used for

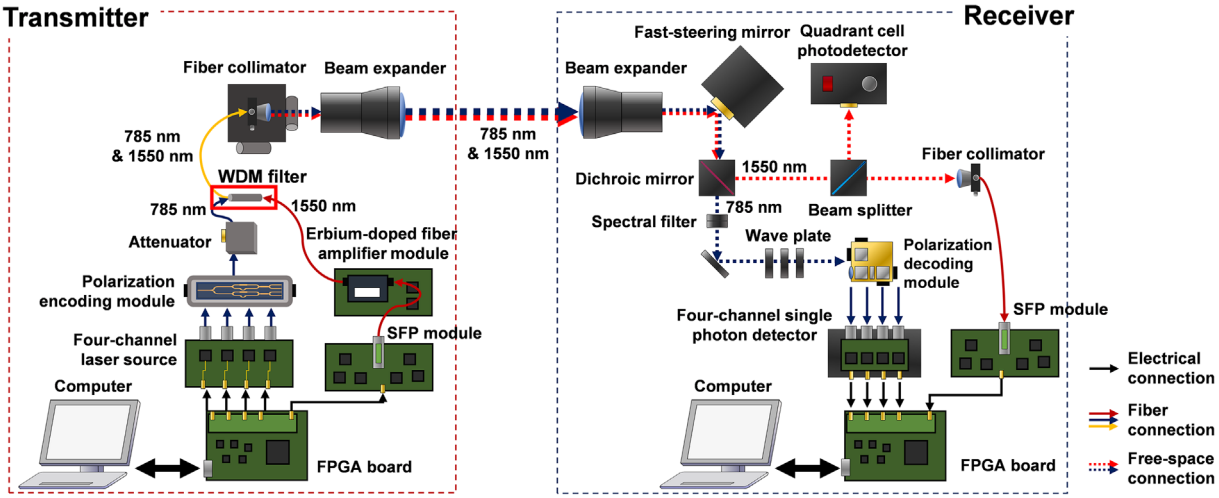

FIGURE 1 Configuration of proposed free-space quantum key distribution (QKD) system. Blue and red arrows indicate 785-nm quantum signal and 1550-nm synchronization signal, respectively.

its verified security. The transmitter generates the signals required for the QKD and transmits them to free space. The receiver receives these signals and separates them using the internal optical components. The signals are then sent to the electrical components, where they are detected and processed accordingly.

Beam-tracking and synchronization channels were used in addition to the quantum channel to implement the system. A quantum channel is a signal channel that delivers quantum key information by transmitting single photons carrying polarization-encoded data. The operating wavelength of the quantum channel was selected as 785 nm, owing to its good atmospheric transmission characteristics and availability for high-performance silicon single-photon detectors (SPDs).

The beam-tracking channel is used as an auxiliary signal to track the position and stabilize the beam, such that the quantum signal can maintain its alignment between the transmitter and receiver. This is necessary because fluctuations in the beam position are inevitable in free-space QKD systems, owing to physical vibrations, atmospheric turbulence, and moving environments. Beam tracking consists of coarse tracking for aligning the system over a wide range and fine tracking for precise alignment and beam stabilization.

A synchronization channel is also used to synchronize the clock and timing of the keys between the transmitter and receiver. This is required because some of the transmitted keys must be compared between the transmitter and receiver to measure the error rate of the communication. We used a single signal to perform both synchronization and beam tracking by splitting it using a free-space beam splitter on the receiver side. We selected a 1550 nm wavelength because of its good atmospheric transmission characteristics and availability for various commercial devices that can be used for signal modulation and amplification. The proposed system and signals are described in detail in the following subsection.

2.1 | Free-space QKD transmitter

The proposed free-space BB84 QKD transmitter consists of the following parts: quantum signal generation, synchronization signal generation, optical components, including a WDM filter, and driving electronics, including a field-programmable gate array (FPGA) board, as shown in Figure 1.

The quantum signal generation part consists of a four-channel laser source that creates a four-channel optical pulse, a polarization-encoding module for encoding the polarization to each channel and combining them, and a variable optical attenuator (VOA) to attenuate the polarization-encoded optical pulses to the single-photon level. By operating only one randomly selected laser at each time slot, an optical pulse with one of four possible polarizations (horizontal H, vertical V, diagonal D, or anti-diagonal A) was generated.

A four-channel laser was fabricated using four distributed feedback laser modules. The modules were operated by gain switching, enabling a high repetition rate and narrow pulse width of less than 100 ps. The temperatures of the modules were controlled separately to obtain an identical center wavelength of 785 nm with a full-width-at-half-maximum of 0.36 nm.

The polarization-encoding module set the polarization of each optical pulse from the four-channel laser source and combined them into a single-mode fiber. The silica

chip used for the module was fabricated by applying a thin-film half-wave plate to Mach–Zehnder interferometers comprising birefringent waveguides and multimode interferometers. Hence, the four polarizations (H, V, D, and A) used in the BB84 protocol could be generated with polarization extinction ratios greater than 18 dB.

Using this polarization-encoding chip, four polarized signals could be generated and combined in a small 80 mm × 20 mm module by simply connecting the optical fibers. Figure 2 shows photographs of the optical components of the transmitter with the four-channel laser source and polarization-encoding module.

The transmitter system operates as follows: The computer generates a random number sequence with a random bit sequence and transfers it to the FPGA board. The FPGA board generates and sends an electrical pulse to one of the four-channel light sources in a random sequence and simultaneously generates a bit sequence to drive a small form-factor pluggable (SFP) transceiver module.

The output optical pulse of the four-channel light source is connected to the polarization-encoding module via a set of polarization-maintaining optical fibers. The module first sets the polarization of the entered light pulse and then combines all the channels into a single waveguide. The light pulse exiting the module is sent to a single-mode optical fiber and attenuated to the single-photon level at the VOA.

The 1550-nm synchronization signal generated at the SFP transceiver module is amplified using a compact erbium-doped fiber amplifier module. The generated 785-nm quantum signal and 1550-nm synchronization signal then enter the input ports of the WDM filter to be multiplexed and sent to a single HI780 fiber.

Finally, the multiplexed signal is sent to a fiber collimator and expanded using a beam expander. All signals are merged using simple fiber connections to address the issues of bulk-optic-based internal free-space alignment configurations.

2.2 | WDM filter design and performance

A WDM filter can receive two optical signals with different wavelengths from two different ports and combine them into one output port. Alternatively, it can receive two optical signals with different wavelengths from one port and separate them through two output ports. The combining operation is called multiplexing, and the splitting operation is called demultiplexing.

In this study, a custom-made WDM filter was used to multiplex the 785-nm quantum channel and 1550-nm synchronization channel inside a free-space QKD transmitter system. By using a WDM filter instead of a conventional dichroic mirror, the spatial modes of the signals could be automatically matched without requiring an alignment process.

Figure 3A shows the structure of the WDM filter. At its output port, the 785-nm quantum signal must be transmitted in single mode to maintain the orthogonality

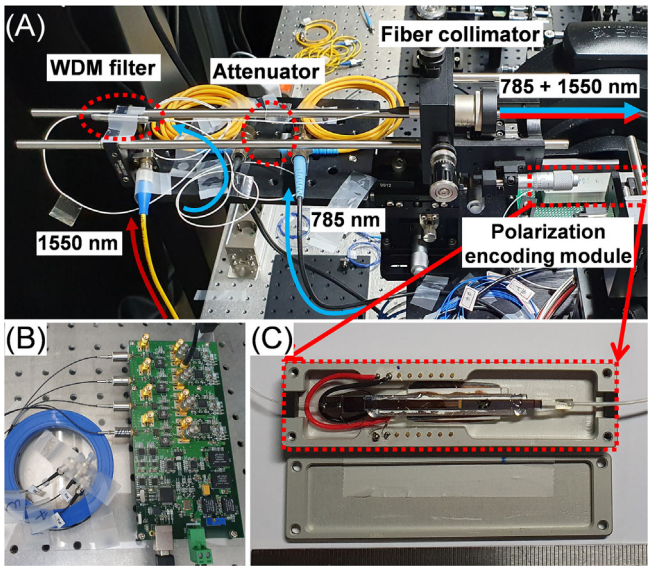

FIGURE 2 Photographs of (A) proposed quantum key distribution (QKD) transmitter system, (B) four-channel laser source, and (C) polarization-encoding module.

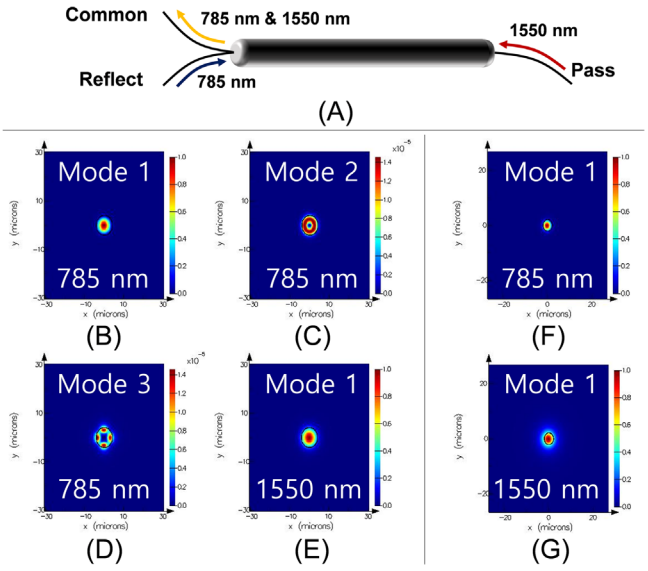

FIGURE 3 (A) Structure of designed wavelength-division multiplexing (WDM) filter. Results of propagating-mode simulation for (B), (C), (D) 785 nm and (E) 1550 nm in a SMF-28 fiber. Results of propagating-mode simulation for (F) 785 nm and (G) 1550 nm in an HI780 fiber.

of the polarization states. For the 1550-nm synchronization signal, single-mode operation is also advantageous for matching the spatial mode with the quantum signals for long-distance transmissions. In other words, single-mode transmission is required for both the 785 and 1550 nm wavelengths in the output common-port fiber of the WDM filter.

Figure 3B–G shows the finite-difference time-domain simulation results for possible spatial modes in the SMF-28 and HI780 optical fibers when the 785 and 1550 nm wavelengths were excited. As shown in Figure 3B–D, the 785 nm signal can propagate in multiple modes in the SMF-28 fiber because its cutoff wavelength is 1260 nm.

As shown in Figure 3E, the 1550 nm signal can only propagate in a single mode in the same fiber. In contrast, in the HI780 fiber, both the 785 and 1550 nm optical signals can only propagate in single mode with different mode sizes, as shown in Figure 3F,G.

Figure 4 shows the measured spatial-mode distribution of the optical signals obtained using an infrared image sensor. Figure 4A,B shows the measured spatial-mode distributions of the optical signals in the SMF-28 optical fiber. In Figure 4A, the elliptical beam shape of the 785 nm signal changes when the fiber is bent, unlike the 1550 nm signal depicted in Figure 4B, which propagates in single mode in the SMF-28 fiber. This observation aligns with the simulation results, confirming that the 785 nm signal propagates in a multimode in the same fiber.

Figure 4C,D illustrates the optical-mode distribution of the signals in the HI780 optical fiber, where both wavelengths operate in single mode. Thus, we used the HI780 optical fiber as the common port for fabricating the device. Notably, the intensity of the 1550 nm signal can be reduced by bending the fiber because the 1550 nm wavelength has a low confinement inside the HI780 fiber, owing to the small core size. Thus, the signal can escape from the core of the fiber when it bends.

To minimize the bending loss of the 1550 nm signal, the fiber length was minimized to 15 cm and well stretched when installed. In addition, an SMF-28 fiber was used as the pass port to receive the 1550 nm optical signal, and an HI780 fiber was used as the reflected port to receive the 785 nm optical signal.

Figure 5 shows the output spectrum from the pass and reflection ports when a broadband light source with wavelengths of 785 nm and 1550 nm was incident on the common port of the WDM filter. The red curve represents the output from the reflected port of the WDM filter. The loss of the 785 nm signal, shown in Figure 5A, was approximately 1.8 dB, and the 1550 nm signal suppression, shown in Figure 5B, was approximately 28.3 dB.

The black curve represents the output from the pass port. The loss of the 1550 nm signal was approximately

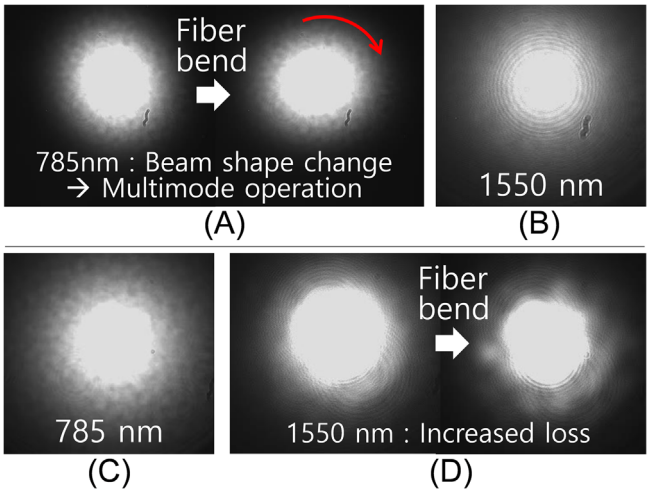

FIGURE 4 Propagated-mode images acquired by infrared image sensor from (A) 785-nm and (B) 1550-nm signals in a SMF-28 fiber. Propagated images acquired from (C) 785-nm and (D) 1550-nm signals in an HI780 fiber.

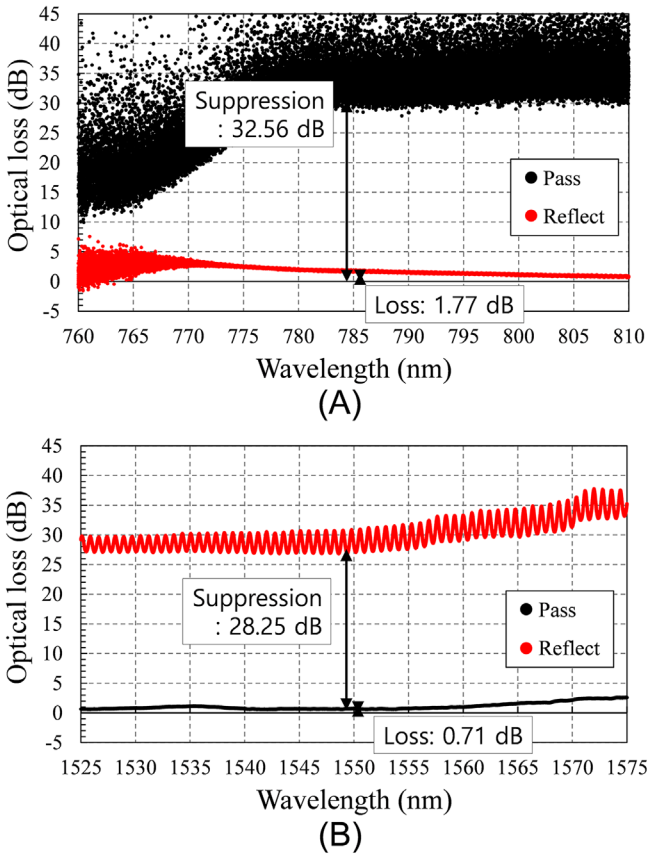

FIGURE 5 Output optical loss measurements from the fabricated wavelength-division multiplexing (WDM) filter at wavelengths of (A) 785 nm and (B) 1550 nm.

0.7 dB, and the suppression of the 785 nm signal was approximately 32.6 dB. Both ports exhibited good performances with low losses and high suppression ratios.

2.3 | Free-space QKD receiver

The free-space QKD receiver consists of the following parts: beam stabilization, synchronization channel, quantum-signal detection, and additional optical and electronic components, as shown in Figure 1.

The beam stabilization and synchronization use the same 1550 nm wavelength signal separated by a 3-dB beam splitter. The beam-stabilization component consists of a fast-steering mirror and quadrant-cell photodetector. A quadrant-cell photodetector is a module in which the detector is divided into four cells. When the optical signal is placed away from the center of the detector cell, the balance between the photocurrents generated by each cell is disturbed. The off-balance is converted into a voltage level, making the module an accurate beam-position detector.

The voltage from the quadrant photodetector is measured using a data-acquisition unit and sent to a computer for control purposes. Specifically, the computer sends a control signal through the data-acquisition unit to correct the dislocation, rotating the fast-steering mirror such that the beam is maintained at the center of the detector cell, thereby compensating for fluctuations and drifts caused by vibrations or turbulence in the system. Thus, the beam-tracking signal is always aligned with the center of the detector cell along with the quantum signal.

The synchronization channel comprises an SFP transceiver module that receives the 1550-nm synchronization signal and sends it to the FPGA board for reference.

The quantum signal detection part consists of a micro-optics-based polarization-decoding module and a silicon-based four-channel SPD, along with optical components, including a set of waveplates for polarization compensation and spectral filters. Figure 6 shows the configuration of the optical components inside the QKD receiver and corresponding beam paths.

The micro-optics-based polarization-decoding module was used to separate the received photons according to their polarization [28]. A 3-dB beam splitter, half-wave plate, and two polarizing beam splitters were installed inside the module to separate the H-, V-, D-, and A-polarized photons. The separated photons were then focused using aspherical lenses with 6.2-mm focal lengths and incident on each multimode fiber with a 62.5-μm core size.

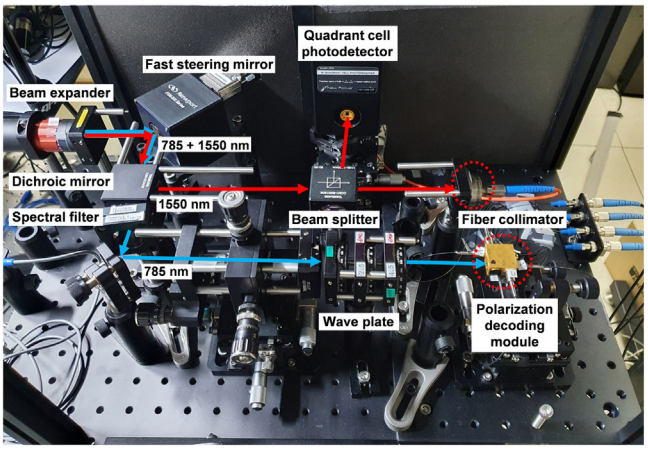

FIGURE 6 Photograph of free-space quantum key distribution (QKD) receiver system. Blue and red arrows indicate 785 nm quantum signal and 1550 nm synchronization signal, respectively.

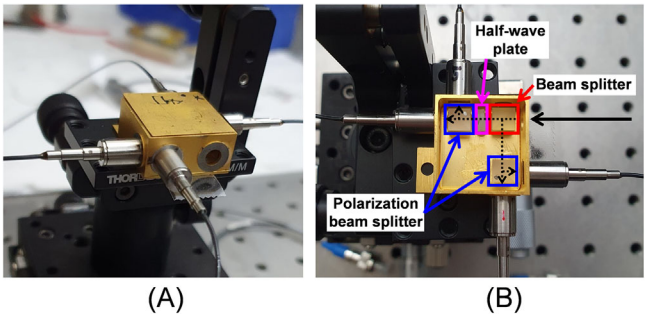

FIGURE 7 Photographs of (A) micro-optics-based polarization decoding module used in proposed quantum key distribution (QKD) receiver system and (B) its configuration.

The measured insertion loss of the single-beam path was less than 5 dB, including the coupling and optical pass losses from the beam splitters. The measured polarization extinction ratio was greater than 22 dB. The dimensions of the module were 65 mm × 65 mm × 11 mm, including the four pre-aligned multimode fibers. The four polarizations can be decoded by aligning the module once, without aligning each fiber. Photographs of the module are shown in Figure 7.

The receiver operated as follows: The diameter of the received optical signal was first reduced to approximately 2 mm using a beam expander and then reflected by a fast-steering mirror. Next, at the dichroic mirror, the 785-nm quantum and 1550-nm signals were split. The 1550 nm optical signal was reflected using a dichroic mirror and then separated using a 3-dB beam splitter for beam stabilization and synchronization.

The reflected half of the signal was incident on the quadrant-cell photodetector and used to stabilize the beam position. The transmitted half was coupled to a multimode fiber using an optical fiber collimator and sent to an SFP transceiver. The optical transceiver converted the received optical signal into an electrical signal and transmitted it to the FPGA board.

The 785-nm quantum key signal was passed through a dichroic mirror and spectral filters. Subsequently, the polarization of the signal was compensated by a set of waveplates and was incident on the micro-optics-based polarization-decoding module. The quantum signal was separated inside the module depending on its polarization, which is the key information. The separated photons were then detected in each channel of the four-channel SPD and converted into electrical pulses.

On the FPGA board, clock synchronization and quantum signal timing analyses were performed using data from the synchronization channel, and electrical pulses from the SPDs were converted into key information. The key rate and QBER were calculated in real time and sent to a computer for monitoring.

3 | SYSTEM PERFORMANCE

The performance of a QKD system can be measured using the key rate and QBER. The key rate refers to the speed of key information distribution between the transmitter and receiver. A higher key rate implies that more key information can be distributed in the same amount of time, thereby enabling higher bandwidth for the encrypted information.

The key rate can be classified into the raw key rate, which is the speed of detection at the receiver, and the sifted key rate, which is counted only when the receiver selects the same basis as the transmitter during detection. The key rate is directly related to the operating speed of

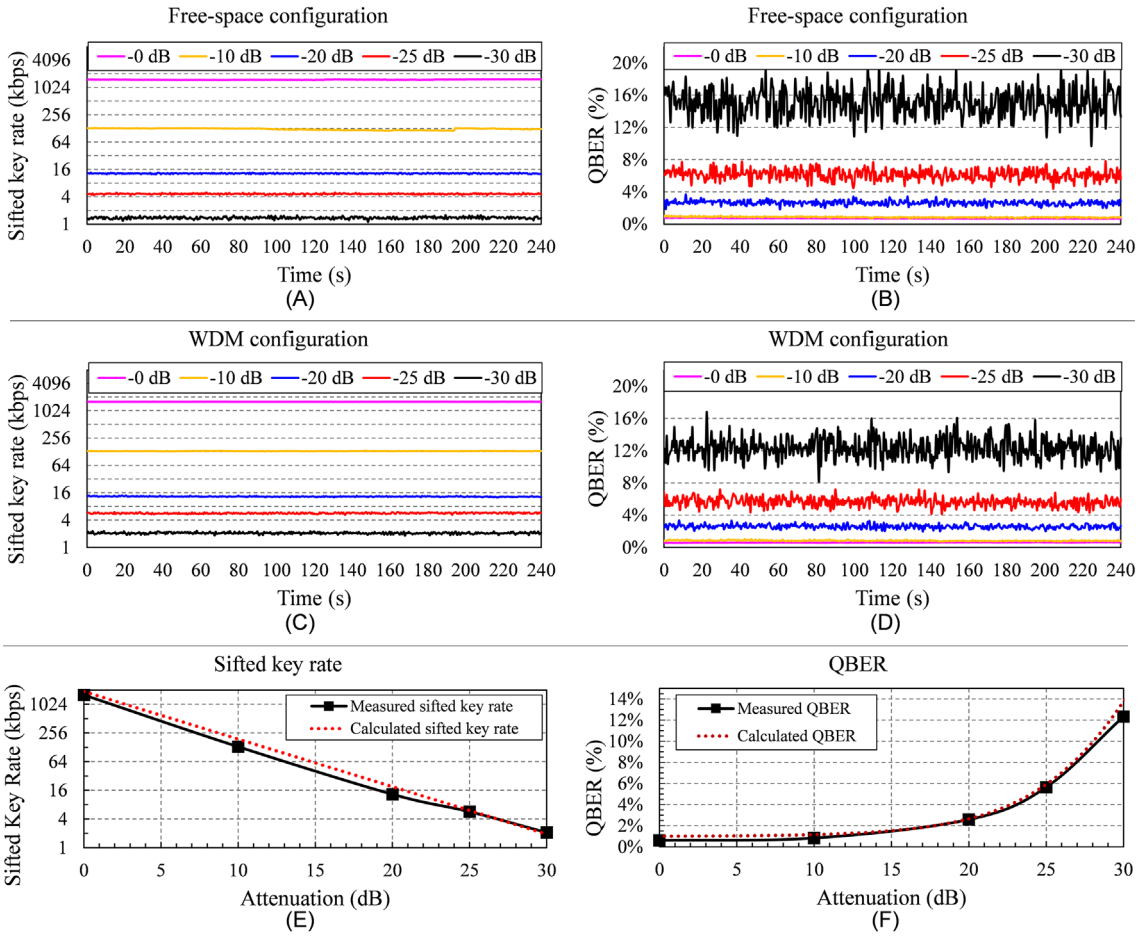

FIGURE 8 Measured (A) sifted key rate and (B) quantum bit error rate (QBER) of conventional bulk-optic component-based transmitter configuration. Measured (C) sifted key rate and (D) QBER of proposed alignment-free transmitter configuration using a wavelength-division multiplexing (WDM) filter. Time-averaged plots of (E) sifted key rate and (F) QBER for attenuation levels.

the system and optical loss of the quantum signal, including the channel loss due to the environment, internal loss inside the receiver system, and detection efficiency of the SPDs.

The QBER quantifies the error rate of the sifted keys. A lower QBER indicates better security because it is inversely related to the amount of information that may have been compromised by eavesdroppers. The QBER can increase because of various factors, including the polarization errors of photons during transmission, noise photons from ambient light, timing errors of quantum signals, false detections from SPDs, and potential eavesdropper attacks.

Because the transmitter and receiver cannot differentiate between the QBER resulting from eavesdropper attacks and those from other sources, it is assumed that all observed QBER is attributable to eavesdropping. When the QBER exceeds 11%, the communication cannot be guaranteed to be secure [1], as this implies that an eavesdropper may have obtained more secret key information than the legitimate parties involved.

The tested QKD system was operated at a speed of 100 MHz, and the quantum signal was attenuated to the average level of 0.1 photons per pulse using a VOA at the transmitter. The distance between the transmitter and receiver was approximately 2.5 m. Additional channel attenuation was applied by placing neutral-density filters at the output of the transmitter to test the performance of the QKD system in lossy environments, which commonly appear at long distances.

Figure 8 shows the measured QBER and sifted key rate according to the channel attenuation. Figure 8A,B shows the sifted key rate and QBER over time for the conventional bulk-optic component-based transmitter, whereas Figure 8C,D shows the same results for the WDM-based transmitter. Figure 8E,F shows the time-averaged sifted key rate and QBER of the measured values from the WDM-based transmitter, according to the additional channel attenuation.

The sifted key rate and QBER of the proposed transmitter system were approximately 1.6 Mbps and 0.62%, respectively. The proposed system showed similar results to the sifted key rate and QBER of 1.5 Mbps and 0.71%, respectively, of a conventional bulk-optic component-based transmitter system. As the channel attenuation increased from 0 to 30 dB, the sifted key rate of the proposed system decreased from 3 Mbps to 3 kbps, matching the calculation results.

In addition, the QBER increased from 0.7% to approximately 12%–15% because of the increased effect of the SPD dark count and ambient light noise as the quantum signal was decreased. In this system, the QBER was expected to reach its theoretical limit of 11% when the additional channel loss was increased to approximately 28 dB.

From the measured key rate and QBER, no considerable difference in the system performance was observed after applying the WDM filter. Moreover, the performance variation under additional channel attenuation agreed with the theoretical estimation, indicating a performance similar to that of the conventional setup using bulk-optic components and free-space alignment.

In this study, a WDM filter was applied to a free-space QKD transmitter system, substantially simplifying the system configuration while maintaining the performance compared with the conventional setup. Notably, performing QKD between distances of more than hundreds of meters is possible if the size of the transmitted beam is adjusted for long-distance transmission by changing the beam expanders.

4 | CONCLUSION

In this paper, we reported on the configuration and evaluated the performance of a free-space QKD transmitter system that did not require internal free-space alignment. The quantum signal was generated using a four-channel laser source emitting 785 nm optical pulses, a chip-based polarization-encoding module for encoding the polarization information for each channel and its integration, and a VOA for attenuating the polarization-encoded optical pulses to the single-photon level.

A custom-made WDM filter was used to multiplex the 785-nm quantum signal with a 1550-nm synchronization signal. Using a polarization-encoding module and WDM filter, the bulk-optic components widely used in conventional QKD transmitters could be replaced in the proposed system, thus eliminating the need for internal free-space alignment.

The insertion loss and isolation of the WDM filter were 1.8 dB and 32.56 dB for 785 nm and 0.7 dB and 28.3 dB for 1550 nm, respectively. The sifted key rate and QBER of the proposed QKD system were approximately 1.6 Mbps and 0.62%, respectively, at an operating speed of 100 MHz. The QBER limit of 11% was estimated to be reached at a channel loss of 28 dB.

The results showed a performance similar to that of a conventional transmitter system that uses bulk-optic components and internal free-space alignment for channel integration. By using a WDM filter for channel integration, the proposed QKD transmitter configuration reduced the system size and avoided the effort required for alignment and spatial-mode matching. This feature is promising for the utilization of QKD in high-speed long-distance applications.

ACKNOWLEDGMENTS

The authors thank Dr. Hae Young Rha for her contribution to the development of real-time data processing using the FPGA.

CONFLICT OF INTEREST STATEMENT

The authors declare that there are no conflicts of interest.

ORCID

Minchul Kim https://orcid.org/0009-0008-1440-0319

REFERENCES

1. P. W. Shor and J. Preskill, *Simple proof of security of the BB84 quantum key distribution protocol*, Phys. Rev. Lett **85** (2000), no. 2, 441.
2. F. Xu, X. Ma, Q. Zhang, L. K. Lo, and J. W. Pan, *Secure quantum key distribution with realistic devices*, Rev. Modern Phys. **92** (2020), no. 2, 025002.
3. S.-K. Liao, H. L. Yong, C. Liu, G. L. Shentu, D. D. Li, J. Lin, H. Dai, S. Q. Zhao, B. Li, J. Y. Guan, W. Chen, Y. H. Gong, Y. Li, Z. H. Lin, G. S. Pan, J. S. Pelc, M. M. Fejer, W. Z. Zhang, W. Y. Liu, J. Yin, J. G. Ren, X. B. Wang, Q. Zhang, C. Z. Peng, and J. W. Pan, *Long-distance free-space quantum key distribution in daylight towards inter-satellite communication*, Nat. Photonics **11** (2017), no. 8, 509–513.
4. S.-K. Liao, W. Q. Cai, W. Y. Liu, L. Zhang, Y. Li, J. G. Ren, J. Yin, Q. Shen, Y. Cao, Z. P. Li, F. Z. Li, X. W. Chen, L. H. Sun, J. J. Jia, J. C. Wu, X. J. Jiang, J. F. Wang, Y. M. Huang, Q. Wang, Y. L. Zhou, L. Deng, T. Xi, L. Ma, T. Hu, Q. Zhang, Y. A. Chen, N. L. Liu, X. B. Wang, Z. C. Zhu, C. Y. Lu, R. Shu, C. Z. Peng, J. Y. Wang, and J. W. Pan, *Satellite-to-ground quantum key distribution*, Nature **549** (2017), no. 7670, 43–47.
5. H. Takenaka, A. Carrasco-Casado, M. Fujiwara, M. Kitamura, M. Sasaki, and M. Toyoshima, *Satellite-to-ground quantum-limited communication using a 50-kg-class microsatellite*, Nat. Photonics **11** (2017), no. 8, 502–508.
6. J. S. Sidhu, T. Brougham, D. McArthur, R. G. Pousa, and D. K. Oi, *Finite key effects in satellite quantum key distribution*, Npj Quantum Inf. **8** (2022), no. 1, 18.
7. J. S. Sidhu, T. Brougham, D. McArthur, R. G. Pousa, and D. K. Oi, *Finite key performance of satellite quantum key distribution under practical constraints*, Commun. Phys **6** (2023), no. 1, 210.
8. A. V. Khmelev, E. I. Ivchenko, A. V. Miller, A. V. Duplinsky, V. L. Kurochkin, and Y. V. Kurochkin, *Semi-empirical satellite-to-ground quantum key distribution model for realistic receivers*, Entropy **25** (2023), no. 4, 670.
9. A. Ntanos, N. K. Lyras, A. Stathis, G. Giannoulis, A. D. Panagopoulos, and H. Avramopoulos, *Satellite-to-ground QKD in urban environment: a comparative analysis of small-sized optical ground stations*, IEEE Aerosp. Electron. Syst. Mag. **39** (2024), no. 6, 16–29.
10. E. Eso, C. Simmons, G. S. Buller, and R. Donaldson, *Impact of visibility limiting conditions on satellite and high-altitude platform quantum key distribution links*, Opt. Express **32** (2024), no. 15, 26776–26792.
11. Ren JG, Abulizi M, Yong HL, Yin J, Li XJ, Jiang Y, Wang WY, Xue HJ, Chen YH, Jin B, Yin YY, *Portable ground stations for space-to-ground quantum key distribution, arXiv preprint*, 2022. DOI 10.48550/arXiv.2205.13828
12. T. Roger, R. Singh, C. Perumangatt, D. G. Marangon, M. Sanzaro, P. R. Smith, R. I. Woodward, and A. J. Shields, *Real-time gigahertz free-space quantum key distribution within an emulated satellite overpass*, Sci. Adv **9** (2023), no. 48, eadj5873.
13. W.-Q. Cai, Y. Li, B. Li, J. G. Ren, S. K. Liao, Y. Cao, L. Zhang, M. Yang, J. C. Wu, Y. H. Li, W. Y. Liu, J. Yin, C. Z. Wang, W. B. Luo, B. Jin, C. L. Lv, H. Li, L. You, R. Shu, G. S. Pan, Q. Zhang, N. L. Liu, X. B. Wang, J. Y. Wang, C. Z. Peng, and J. W. Pan, *Free-space quantum key distribution during daylight and at night*, Optica **11** (2024), no. 5, 647–652.
14. H. Chun, I. Choi, G. Faulkner, L. Clarke, B. Barber, G. George, C. Capon, A. Niskanen, J. Wabnig, D. O'Brien, and D. Bitauld, *Handheld free space quantum key distribution with dynamic motion compensation*, Opt. Express **25** (2017), no. 6, 6784–6795.
15. G. Vest, P. Freiwang, J. Luhn, T. Vogl, M. Rau, L. Knips, W. Rosenfeld, and H. Weinfurter, *Quantum key distribution with a hand-held sender unit*, Phys. Rev. Appl. **18** (2022), no. 2, 024067.
16. J.-P. Bourgoin, B. L. Higgins, N. Gigov, C. Holloway, C. J. Pugh, S. Kaiser, M. Cranmer, and T. Jennewein, *Free-space quantum key distribution to a moving receiver*, Opt. Express **23** (2015), no. 26, 33437–33447.
17. S. Nauerth, F. Moll, M. Rau, C. Fuchs, J. Horwath, S. Frick, and H. Weinfurter, *Air-to-ground quantum communication*, Nat. Photonics **7** (2013), no. 5, 382–386.
18. C. J. Pugh, S. Kaiser, J. P. Bourgoin, J. Jin, N. Sultana, S. Agne, E. Anisimova, V. Makarov, E. Choi, B. L. Higgins, and T. Jennewein, *Airborne demonstration of a quantum key distribution receiver payload*, Quantum Sci. Technol **2** (2017), no. 2, 024009.
19. H.-Y. Liu, X. H. Tian, C. Gu, P. Fan, X. Ni, R. Yang, J. N. Zhang, M. Hu, J. Guo, X. Cao, X. Hu, G. Zhao, Y. Q. Lu, Y. X. Gong, Z. Xie, and S. N. Zhu, *Drone-based entanglement distribution towards mobile quantum networks*, Nat. Sci. Rev. **7** (2020), no. 5, 921–928.
20. H. Y. Liu, X. H. Tian, C. Gu, P. Fan, X. Ni, R. Yang, J. N. Zhang, M. Hu, J. Guo, X. Cao, and X. Hu, *Optical-relayed entanglement distribution using drones as mobile nodes*, Phys. Rev. Lett. **126** (2021), no. 2, 020503.
21. A. Conrad, S. Isaac, R. Cochran, D. Sanchez-Rosales, T. Rezaei, T. Javid, A. J. Schroeder, G. Golba, D. Gauthier, and P. Kwiat, *Drone-based quantum communication links*, In *Quantum Computer, Communication, Simulation III*, Vol. **12446**, SPIE, 2023, p99–106.
22. J.-S. Choe, H. Ko, B. S. Choi, K. J. Kim, and C. J. Youn, *Silica planar lightwave circuit based integrated 1×4 polarization beam splitter module for free-space BB84 quantum key distribution*, IEEE Photonics J. **10** (2018), no. 1, 1–8.
23. H. Ko, J. S. Choe, B. S. Choi, K. J. Kim, J. H. Kim, Y. Baek, and C. J. Youn, *Daylight operation of a high-speed free-space quantum key distribution using silica-based integration chip and micro-optics-based module*, (Optical Fiber Communications Conference and Exhibition, San Diego, CA, USA), 2019, 1–3.

24. H. Ko, B. S. Choi, J. S. Choe, K. J. Kim, J. H. Kim, and C. J. Youn, *Critical side channel effects in random bit generation with multiple semiconductor lasers in a polarization-based quantum key distribution system*, Opt. Express **25** (2017), no. 17, 20045–20055.
25. H. Ko, B. S. Choi, J. S. Choe, K. J. Kim, J. H. Kim, and C. J. Youn, *High-speed and high-performance polarization-based quantum key distribution system without side channel effects caused by multiple lasers*, Photonics Res. **6** (2018), no. 3, 214–219.
26. H. Ko, K. J. Kim, J. S. Choe, B. S. Choi, J. H. Kim, Y. Baek, and C. J. Youn, *Experimental filtering effect on the daylight operation of a free-space quantum key distribution*, Sci. Rep. **8** (2018), no. 1, 1–7.
27. M. Avesani, L. Calderaro, M. Schiavon, A. Stanco, C. Agnesi, A. Santamato, M. Zahidy, A. Scriminich, G. Foletto, G. Contestabile, and M. Chiesa, *Full daylight quantum-key-distribution at 1550 nm enabled by integrated silicon photonics*, Npj Quantum Inf **7** (2021), no. 1, 93.
28. Choi BS, Ko H, Choe JS, Kim KJ, Youn CJ, Kim JH, Baek Y., *Micro-optics based polarization decoding module for free-space quantum key distribution*, (23rd Opto-Electronics and Communications Conference, Jeju, Republic of Korea), 2018. DOI 10.1109/OECC.2018.8729879

AUTHOR BIOGRAPHIES

Minchul Kim received his BS and MS degrees in electrical engineering from the School of Electrical Engineering, Korea Advanced Institute of Science and Technology, Daejeon, Republic of Korea, in 2017 and 2019, respectively. Since 2019, he has been working with the Electronics and Telecommunications Research Institute, Daejeon, Republic of Korea. His research interests include free-space quantum key distribution systems and silicon photonics.

Kyongchun Lim received his BS degree in electrical and computer engineering from the Department of Electrical and Computer Engineering, Sungkyunkwan University, Suwon, Republic of Korea, in 2012, and his MS and PhD degrees in electrical engineering from the Korea Advanced Institute of Science and Technology, Daejeon, Republic of Korea, in 2014 and 2019, respectively. Since 2019, he has been working for the Electronics and Telecommunications Research Institute in Daejeon, Republic of Korea. His major research interests include quantum communications, quantum key distribution, and quantum information processing.

Joong-Seon Choe received his BS, MS, and PhD degrees in physics from the Department of Physics, Seoul National University, Seoul, Republic of Korea, in 1994, 1996, and 2001, respectively. He has been with the Electronics and Telecommunications Research Institute, Daejeon, Republic of Korea, since 2001. His research interests include integrated photonic devices, quantum information, and optical communication.

Byung-Seok Choi received his BS and MS degrees in material science and engineering from Seoul National University, Seoul, Republic of Korea, in 1996 and 1998, respectively, and his PhD in electrical engineering from the Korea Advanced Institute of Science and Technology, Daejeon, Republic of Korea, in 2016. He joined the Basic Research Laboratory, Electronics and Telecommunications Research Institute, Daejeon, Republic of Korea, in 2001, where he has been engaged in the research and development of various devices for fiber optics and quantum key distribution systems. His current research interests include the design, characterization, and fabrication of entanglement-based quantum networks.

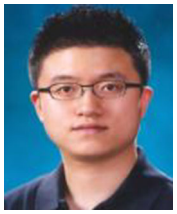

Kap-Joong Kim received his PhD degree in physics from the Korea Advanced Institute of Science and Technology, Daejeon, Republic of Korea, in 2014. He is currently a senior researcher with the Electronics and Telecommunications Research Institute, Daejeon, Republic of Korea. His research interests include the design, fabrication, and characterization of silicon-based integrated quantum-photonic devices and quantum light sources.

Ju Hee Baek received her BS degree from the Department of Electrical Engineering Education at Chungnam National University, Daejeon, Republic of Korea, in 2006. She currently works at the Quantum Technology Research Department of the Electronics and Telecommunications Research Institute, Daejeon, Republic of Korea. Her research interests include optical alignment, measurement, and packaging.

Chun Ju Youn received his PhD degree in electronics engineering from the Korea Advanced Institute of Science and Technology, Daejeon, Republic of Korea, in 2003. From 2003 to 2005, he was a principal researcher at the Samsung Advanced Institute of Technology, Suwon, Republic of Korea, where he worked on an optical internet network. Since 2005, he has been with the Electronics and Telecommunication Research Institute, Daejeon, Korea, where he is currently an assistant vice president of the Quantum Technology Research Division. His current research interests include quantum communication, quantum optics, quantum technologies, and optical communication.

How to cite this article: M. Kim, K. Lim, J.-S. Choe, B.-S. Choi, K.-J. Kim, J. H. Baek, and C. J. Youn, *Free-space quantum key distribution transmitter system using WDM filter for channel integration*, ETRI Journal **46** (2024), 806–816, DOI 10.4218/etrij.2024-0142.